2020

Quantum Defect Measurements for High Angular Momentum Rydberg States of Potassium

Abraham Hill
Colby College

Quantum Defect Measurements for High Angular Momentum Rydberg States of Potassium

Abraham Hill

A thesis presented to the faculty of the

Department of Physics and Astronomy at

Colby College

Department of Physics and Astronomy

Colby College

Waterville, ME

May, 2020

Abstract

We report measurements of the quantum defect for the *f*-, *g*-, and *h*-states of potassium with principal quantum number *n* between 26 and 29. Ground state potassium atoms in a magneto-optical trap are excited from the 4*s* state to the 5*p* state, then from the 5*p* state to the nd_j state using lasers at 405nm and 980nm, respectively. We then measure the millimeter wave frequencies of the nd_j to *nl* transitions. We extract the quantum defects from these frequency measurements in conjunction with the known *d*-state quantum defects. Experimental challenges with fully canceling the electric field and the inhomogeneity of the electric field inside the magneto-optical trap lead to our greatest sources of uncertainty. Our measurements show significant disagreement with predicted values that are calculated from the theoretical dipolar and quadrupolar polarizabilities of potassium.

Acknowledgements

I would like to thank Professor Charles Conover for sharing a small piece of his research with me by giving me the opportunity to work in his lab. Professor Conover's guidance, support, and patience throughout this project enabled me to learn a great deal and grow as a physicist.

I would like to thank the Colby College Department of Physics and Astronomy. The incredible professors I have had in my time at Colby have challenged me, helped me grasp difficult and interesting topics, and inspired in me a love for physics that I will take with me and continue to nurture in my years after Colby.

I would like to thank my fellow physics classmates for their friendship, camaraderie, and humor. For me, Mudd was like a second home on campus, and some of my most cherished memories are from working late on problem sets there with friends.

I would like to thank my parents, Mary and Paul, my grandparents, Mary and Bob, and my siblings, Oscar and Ruby, for their unconditional support and encouragement. I consider myself very lucky to have such great family. This thesis is dedicated to Bob ("GrandPa") who passed away in April.

Contents

1 Introduction

1.1 Rydberg Atoms

A Rydberg atom is any atom that contains at least one electron that has been excited to a state with high principal quantum number. These highly excited electrons have orbits than extend far beyond ground state atoms.

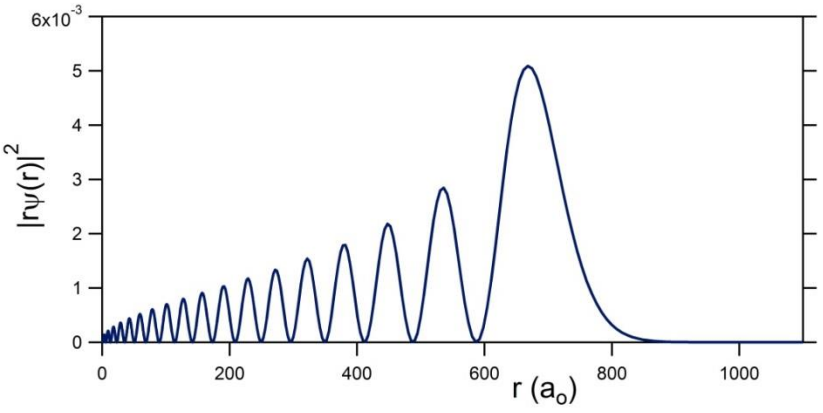

Figure 1: Radial probability distribution for the 20p state of hydrogen. The size of this Rydberg state is two orders of magnitude larger than the ground state.

Figure 1 shows a sample probability distribution of a Rydberg atom. It is clear that the electron is overwhelmingly likely to be found hundreds of Bohr radii away from the nucleus in a Rydberg atom with principal quantum number of 20, whereas ground state atoms have sizes of on the order of a single Bohr radius. The classical picture of a Rydberg atom is an electron in a large orbit around the nucleus or core. This model tells us that the electron moves very slowly when it is far from the center of the atom, which provides further insight into the reason why the electron is most likely to be found far away.

The fact that Rydberg atoms have highly excited electrons means that they have low binding energies. Since the energy of the electron goes as one over the principal quantum

number squared, when n is large, the energy can be very close to zero, so it takes less energy to ionize Rydberg atoms than it does for atoms with lower principal quantum number.

1.2 The Quantum Defect

Alkali atoms are often called "hydrogenic" because they consist of a single valence electron bound to a positively charged core containing the nucleus as well as a "cloud" of electrons in full valence shells. For that reason, the energy levels of alkali atoms are very similar to that of hydrogen. However, the central ion is more complex than the single proton in a hydrogen atom. The inner electron cloud has a radius on the order of one Bohr radius, which is much larger than a single proton. In addition, the core is polarizable because it is not a rigid object. These differences give rise to slight changes in the energies of alkali atoms, so that their energies are described by the following equation,

$$E = -\frac{hcR}{(n-\delta_l)^2} \qquad (1)$$

where h is Planck's constant, c is the speed of light, R is the Rydberg constant, and δ_l is the quantum defect, which accounts for the differences between a proton and the ion at the center of alkali atoms [1].

The quantum defect is a function of the azimuthal quantum number, l, which describes the angular momentum of an atom. The classical picture of an orbit with low angular momentum is that the orbit is more eccentric; the electron passes close to the nucleus before being accelerated away in a loop that is more linear than circular. For higher angular momentum states, the orbit is more circular. Although quantum mechanics specifies that the electron's motion is not so well defined, the classical picture is useful in understanding the reason why the electron has a higher probability of being found close to the nucleus for low angular momentum states.

For alkali atoms, since the central ion has significant size, a valence electron with low angular momentum ($l < 4$) can actually penetrate the inner electron cloud. This significantly alters the energy of the electron since it experiences a much stronger attractive potential when inside the cloud. The penetration of the electron into the cloud is the dominant reason for the quantum defect for lower angular momentum states. For high angular momentum states, the electron has a very low probability of entering the cloud, but there is still a quantum defect for a different reason. The central ion is composed of the positively charged nucleus and the negatively charged electrons, which can move in relation to each other. The ion is susceptible to being polarized by the valence electron because the electron cloud "feels" a repulsive electrostatic force while the nucleus feels an attractive one. In turn, the valence electron experiences a slightly stronger attractive potential than it would if it were orbiting a single proton because the positive charge in the ion is closer than the negative charge, on average. In addition to this dipole polarizability, the ion can be polarized in a quadrupole. This polarization changes the electric potential of the ion, and therefore the energy levels of the atom. The modification to the energy levels is parametrized by the quantum defect, which depends on the dipole and quadrupole polarizabilities α_d and α_q, respectively:

$$\delta = n^3 \frac{\alpha_d}{2} \langle 1 / r^4 \rangle + n^3 \frac{\alpha_q}{2} \langle 1 / r^6 \rangle \quad (2)$$

The radial expectation values $\langle r^{-4} \rangle$ and $\langle r^{-6} \rangle$ are well approximated by those of hydrogen, which can be calculated for given n and l [2, 3]. The correlation between energy levels of alkali atoms and their core polarizabilities has been known since 1933 [4]. The quantum defect due to core polarizability is dominant in states that have azimuthal quantum number of three or greater. This thesis focuses on measurement of states with azimuthal quantum number 3, 4, and 5, often

referred to as the *f*, *g*, and *h* states respectively. As such, the quantum defect we are measuring is due to core polarizability, not core penetration.

1.3 Measuring the Quantum Defect

In order to measure the quantum defect for *f*-, *g*-, and *h*-states of potassium, we take advantage of the fact that the quantum defects for the *d*-states, with azimuthal quantum number of two, are well known. For a given principal quantum number *n*, we excite the atoms to the *nd* state with lasers, then drive the transitions to the *nf*, *ng*, and *nh* states and measure the frequency required to do so. The same method for extracting the defect is used for all three states, so for simplicity I will refer to these states as *nl*. The difference in energy between the *nd* and *nl* state is

$$\Delta E = h\nu_{dl} \quad (3)$$

where ν_{dl} is the measured frequency of the photon used to drive the transition. We also know that the energy of each state is described by equation (1), so taking the difference, we get

$$h\nu_{dl} = -\left(\frac{hcR}{(n-\delta_l)^2} - \frac{hcR}{(n-\delta_d)^2}\right) \quad (4)$$

Solving for δ_l yields the result

$$\delta_l = n - \sqrt{\frac{cR}{\frac{cR}{(n-\delta_d)^2} - \nu_{dl}}} \quad (5)$$

So, by measuring the frequency of the photon that drives the transition, we can determine the quantum defect. For $n = 27$, ν_{dl} is about 90400 MHz, which corresponds to a wavelength of 3.3 millimeters.

Additionally, the uncertainty in the l-state quantum defect σ_l follows directly from the uncertainties in the measured frequency σ_ν, and d-state quantum defect σ_d according to the relation:

$$\sigma_l^2 = \left(\frac{\partial \delta_l}{\partial \nu}\right)^2 \sigma_\nu^2 + \left(\frac{\partial \delta_l}{\partial \delta_d}\right)^2 \sigma_d^2 \quad (6)$$

where ν_{dl} is written as ν to simplify the notation [5]. Using equations (5) and (6), we can extract the quantum defects of high angular momentum Rydberg states and their uncertainties from frequency measurements of the photons that drive the transitions between states.

2 Experiment

2.1 Experimental Overview

Potassium atoms are heated to a gas and injected into the vacuum chamber of a magneto-optical trap (MOT), in which a pressure of 5 x 10^{-9} Torr is maintained. The MOT uses Doppler cooling and an external magnetic field to reduce the speed of the atoms and confine them in a dense cloud in the center of the chamber. The cloud contains about 5 x 10^{6} atoms with a temperature of one to two mK and has diameter of 0.5mm [1]. Lasers are shone though the cloud in order to excite the atoms to Rydberg states. This is laser excitation is done in two stages because any transition in which the azimuthal quantum number changes by more than one is forbidden by quantum mechanics. In order to get from the ground state ($4s_{1/2}$) to our initial Rydberg state ($nd_{5/2}$) we have to change l by two, so an intermediate step is necessary.

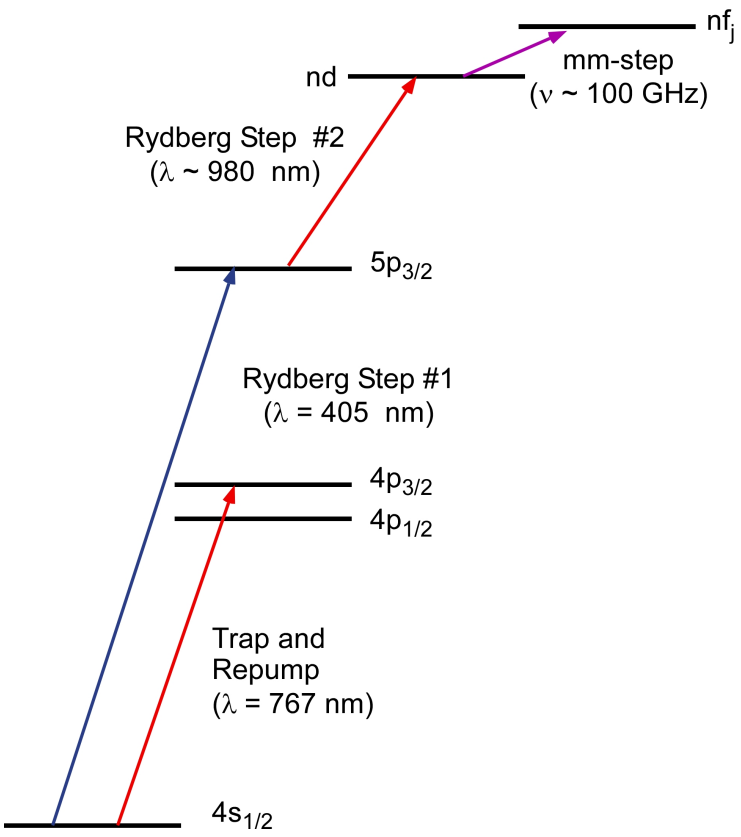

Figure 2: The multi-step laser excitation of potassium atoms to Rydberg states. All lasers in this experiment are external cavity diode lasers.

As shown in Figure 2, a 405nm laser excites the ground state atoms to the intermediate $5p_{3/2}$ state. From there, the atoms are further excited by a 980nm laser to the initial Rydberg state. Next, the millimeter wave source drives the transitions to high angular momentum states. These high angular momentum Rydberg atoms are then ionized using an electric field, which also accelerates the free electrons to a microchannel plate detector. In order to maintain a population of atoms in the initial state to transition to high angular momentum states, the excitation and detection is done in short, sequential pulses and repeated many times. One iteration of this sequence takes only about 8 microseconds (Figure 3).

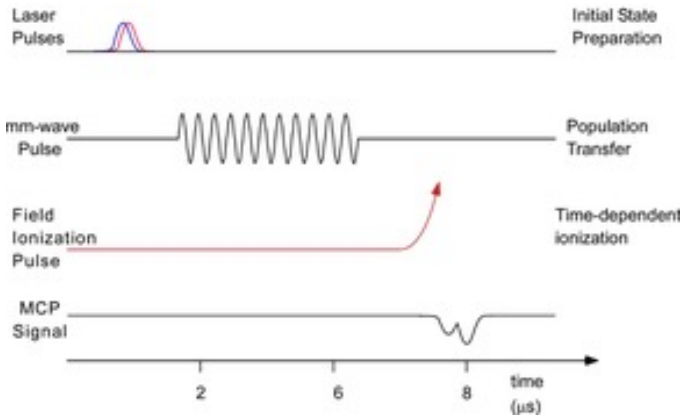

Figure 3: The sequential excitation of the experiment. The lasers excite potassium atoms in the cloud to Rydberg states, then transitions between states are driven by the millimeter wave pulse. Next, the atoms in the final state are ionized by an electric field and the electrons are accelerated to the detector. This process is repeated as the millimeter wave source scans over a range of frequencies.

This repetition also allows for scanning of the millimeter wave source's frequency in order to find the frequency where the microchannel plate signal is the strongest. That frequency therefore produces the most Rydberg atoms in the high-*l* state and is the one that most accurately drives the transition between states.

2.2 Millimeter Waves

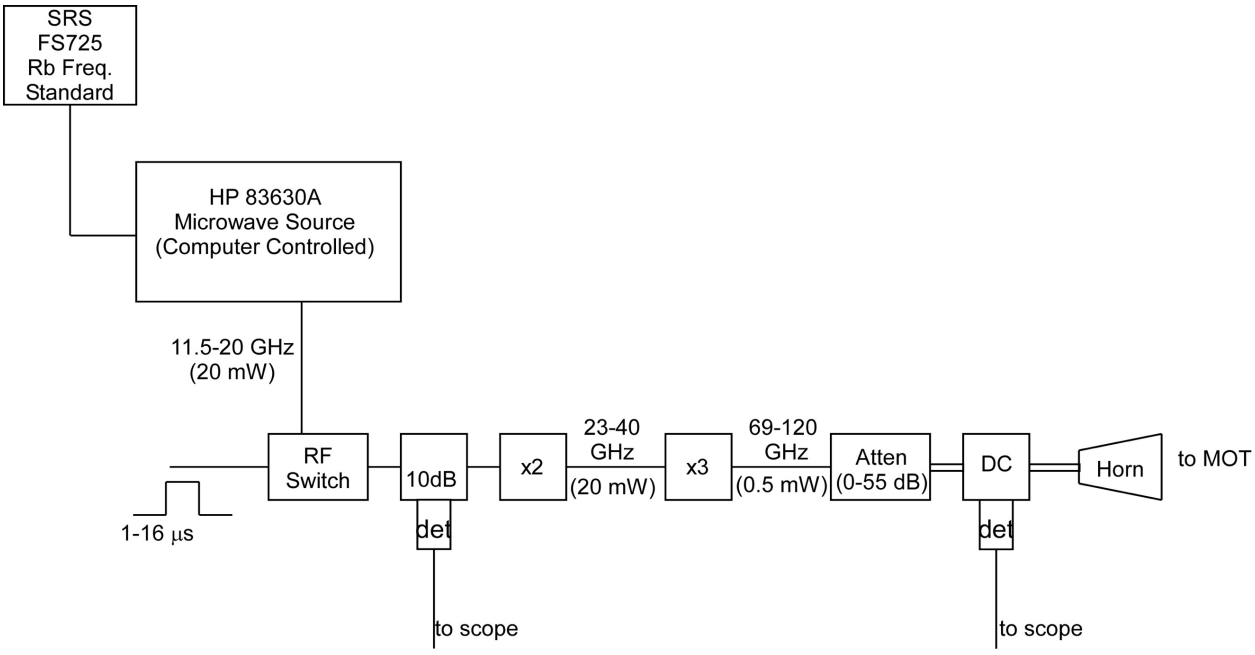

Figure 4: The millimeter wave source for driving transitions between Rydberg states.

The source for millimeter light waves (Figure 4) consists of an SRS 725 Rb Frequency Standard, which generates a frequency of 10^{10} Hertz, setting the uncertainty in the frequency at one part in 10^{10}. A Hewlett-Packard microwave oscillator creates light waves at microwave frequencies. Next, the waves go through an RF switch which lets the microwave pulse through after the laser pulse is over. This is followed by a 10 dB coupler that sends 10% of the power to a detector so that the output of the RF switch can be monitored. The remainder of the power goes through an active frequency doubler, then a passive frequency tripler, so that the frequency is multiplied by six in total and the waves go from microwave to millimeter wave frequency. The millimeter waves then go through a variable attenuator, which can further reduce the power of the waves as necessary, and a directional coupler to another detector to monitor the waves. Finally, the waves are sent into a horn which launches them into the MOT.

In order to produce the clearest signal, it is important to adjust the power of the millimeter waves using the attenuator. If the power is too high, the transition between states can

be driven so strongly that it can occur across a wide range of frequencies, which makes it more difficult to determine the actual frequency of the transition. This phenomenon is called "power broadening." If the power is too low, on the other hand, it can be difficult to distinguish the signal from noise coming into the detector, which also introduces uncertainty. A power that strikes the correct balance is one that induces a small amount of power broadening but produces a clear signal. This balance is found experimentally for each transition.

The lab computer controls the microwave source to set the frequency for each experiment. In order to scan over a range of frequencies, we control the output of the microwave source to be the sum of two frequencies: the base frequency, which is held constant, and the offset frequency, which is varied. Usually we choose the base frequency to be close to the frequency of the transition if the quantum defect was zero so that we can observe the impact of the quantum defect on the transition frequency. The output frequency is therefore described by the relation

$$\nu_{output} = 6 \times \left(\nu_{base} + \nu_{offset}\right) \quad (7).$$

2.3 Field Ionization and Detection of Rydberg States

Once the millimeter wave pulse occurs, the goal is to determine whether that pulse frequency successfully drove the transition between Rydberg states that we are trying to measure. To do this, we turn on a selectively tuned electric field in order to ionize atoms in the high angular momentum Rydberg state, but not those in the initial Rydberg state. The electric potential *V* of a Rydberg atom is well approximated by the potential of the hydrogen atom in 1-D

$$V = -\frac{ke}{|z|} \quad (8)$$

where k is the Coulomb constant, e is the electron charge, and z is the distance of the electron from the nucleus [1]. This potential binds the electron to the nucleus as long as the electron has less energy than the maximum value of the potential. When an external electric field of magnitude E is applied, a new potential energy $V = -Ez$ is added to the system. This addition "tilts" the electric potential of the system, allowing some electrons to escape (Figure 5).

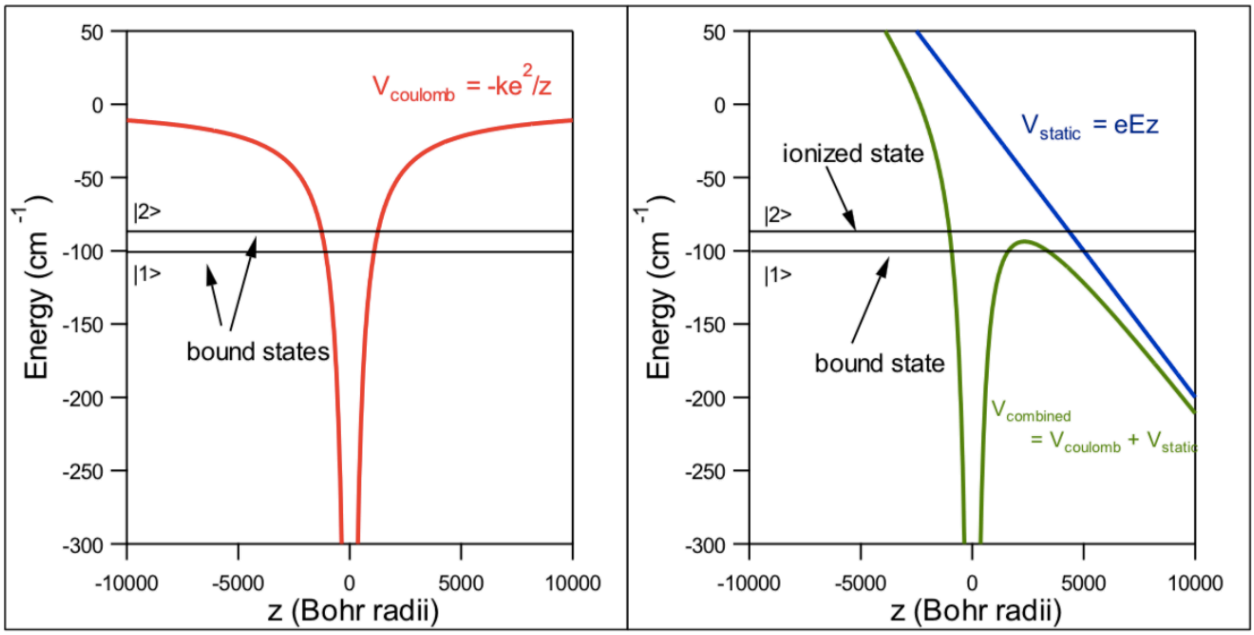

Figure 5: Left: the potential energy of the electron with no electric field, approximated by the Coulomb potential. Right: applying the electric field (blue) "tilts" the potential energy of the system. Selectively tuning the magnitude of the electric field allows for ionization of the final Rydberg states.

By ramping up the magnitude of this external field, we ionize the final state atoms at a different time than the others because of the difference in energy between the two states [1]. This way we can determine how many of the detected electrons came from atoms in the final state of the millimeter wave transition.

The same electric field that ionizes the atoms also accelerates the now free electrons to a microchannel plate detector, which amplifies the signal and converts it to a voltage, which is then displayed on an oscilloscope as a function of time (Figure 6).

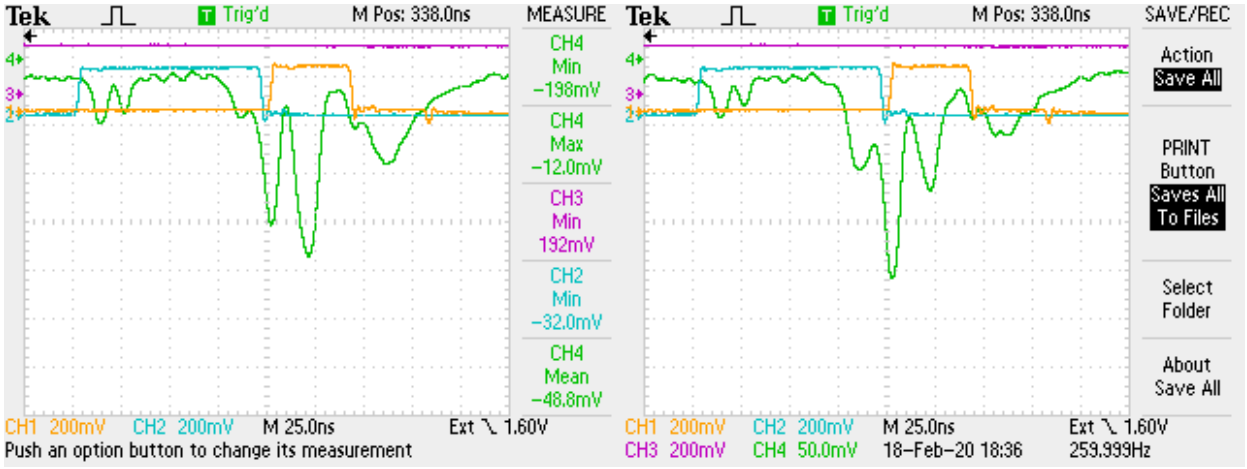

Figure 6: Oscilloscope traces for the 27d to 27g transition in potassium. The horizontal axis is time and the vertical axis is voltage from the detector. Left: output for a millimeter wave frequency that does not drive the transition. Right: output with the correct frequency. The ionization signal appears just left of the center under the blue gate.

When the correct Rydberg state is produced, a clear voltage drop appears on the oscilloscope at the specific time that that state is ionized. The magnitude of the voltage drop corresponds to the number of atoms that made the desired transition for a given millimeter wave frequency. An SP250 gated integrator calculates the total area underneath the green curve in the oscilloscope trace for each frequency. This data is processed by an Igor software program that subtracts the noise and creates a spectrum of the amount of signal for the range of frequencies scanned by the

millimeter waves (Figure 7).

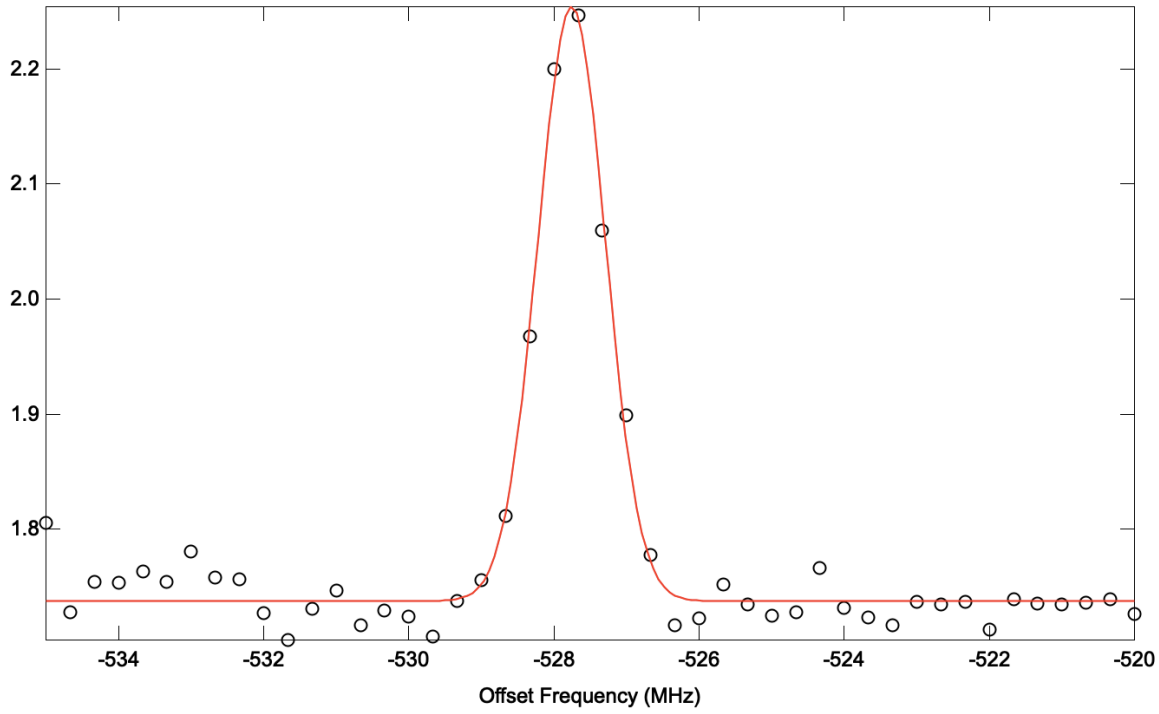

Figure 7: Spectrum of the 28d to 28f transition with Vsum = -14.6 V, ΔV = -10 V, and Vy = 4 V (see Figure 8). The data (black) fit a Gaussian profile (red) which is used to find the frequency at which the signal is greatest.

The spectrum shows a large spike in signal at the frequency that drives the transition. Applying a Gaussian fit to the spectrum allows us to precisely determine that frequency.

2.4 Electric Field Nulling

An external electric field can shift the energy levels of atoms due to the Stark effect. The amount of the shift is proportional to the square of the magnitude of the electric field [3], so that

$$\nu = \nu_0 - \frac{\Delta\alpha}{2} E_{net}{}^2 \qquad (9)$$

where E_{net} is the magnitude of the electric field, ν is the frequency of the transition, ν_0 is the zero-field frequency of the transition, and $\Delta\alpha$ is the difference in polarizabilities between the two states. Rydberg states of potassium are susceptible to this shift, so it is important that our

measurement is conducted as close to zero field as possible. However, due in large part to the microchannel plates, which operate at 1850 Volts, a stray electric field does exist inside the MOT. This field leads to the greatest source of uncertainty in our measurements. In order to cancel these stray fields as much as possible, static voltages are applied to rods inside the vacuum chamber (Figure 8).

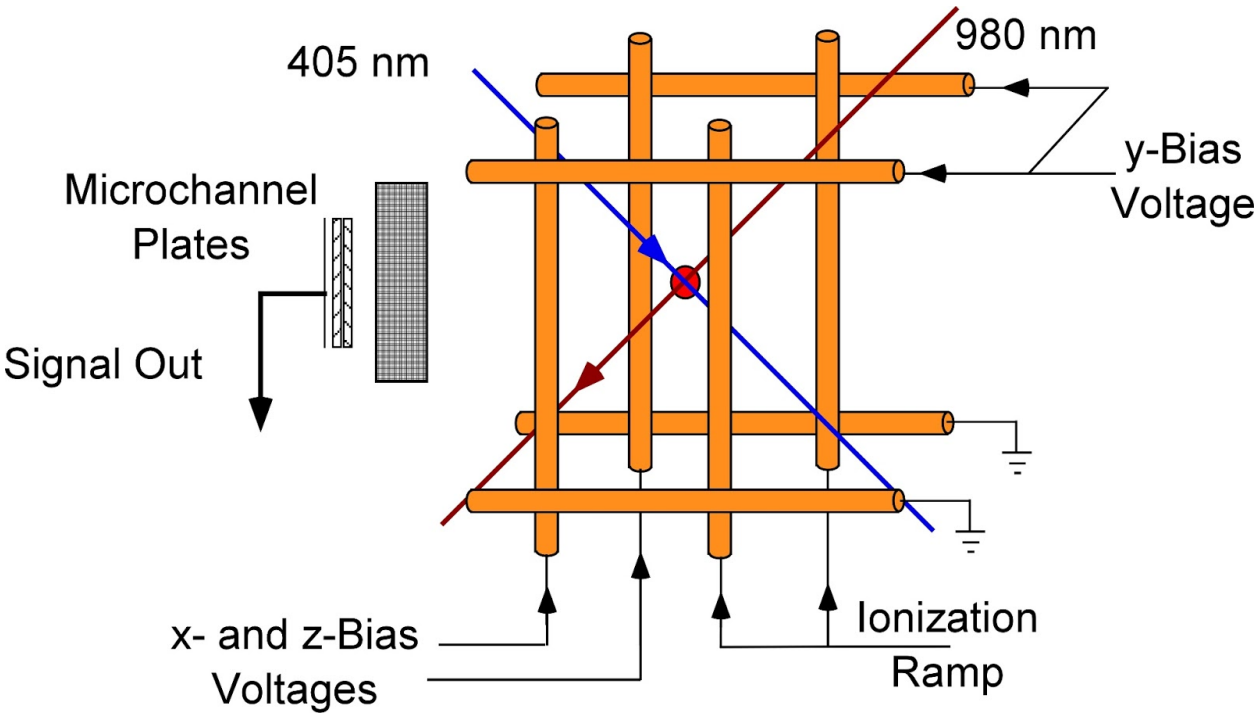

Figure 8: Applying static voltages to rods inside the vacuum chamber in order to cancel stray electric fields in the x, y, and z directions. Nulling the electric field neutralizes the impact of the Stark effect on the energy levels of the Rydberg atoms.

In the figure, the z-axis is right/left, the y-axis is up/down, and the x-axis is in/out of the page. The electric field in the y-direction is canceled by adjusting the magnitude of the voltage (V_y) in the top two horizontal rods. The field in the z-direction is canceled by adjusting the magnitude of the *sum* of the voltage (V_{sum}) in the two leftmost rods, and the field in the x-direction is canceled the adjusting the magnitude of the *difference* in voltages (ΔV) between those same two rods. The two rightmost rods are used to ionize atoms in the final Rydberg state and accelerate the free electrons to the microchannel plate detector. This method for canceling the field does not create a

homogenous field inside the MOT, but rather it nulls the field at a single point. Moving in any direction away from this point upsets the balance of the voltages applied to the rods because the electric field is a function of the distance away from the rods. The cloud of trapped atoms in the vacuum chamber is very small: its effective size is the volume created by the intersection of the laser beams, each of which has 100 μm diameter. While it is small, the cloud's size is significant, so inhomogeneity of the electric field is a source of uncertainty in this measurement because it is impossible to cancel the field for every atom.

The stray electric field inside the MOT shifts over time, so the voltages applied to counteract it must be adjusted for each frequency measurement. In order to find the voltages where the field is zero, we take multiple frequency measurements of the same transition, changing the applied voltage in one direction at a time. For example, we take multiple measurements with different values of V_{sum} while holding ΔV and V_y constant, then more

measurements while changing ΔV, and finally we do the same for V_y.

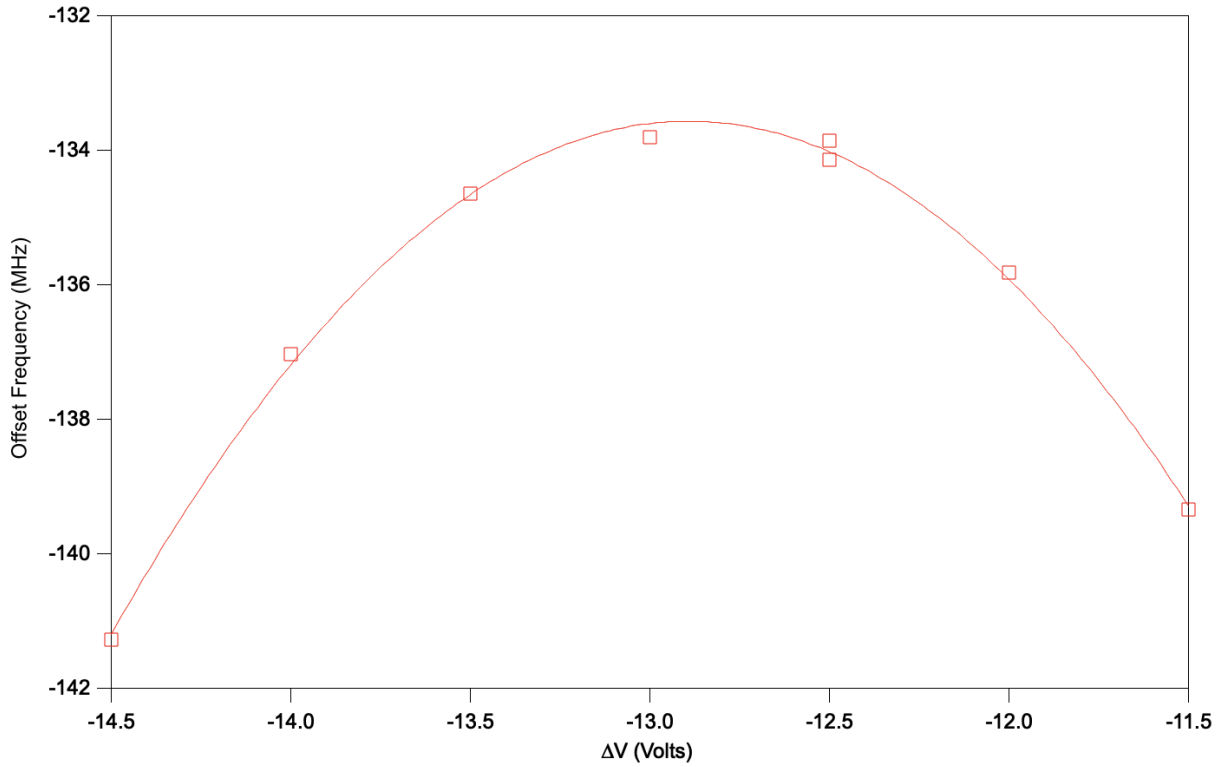

Figure 9: A plot of frequency versus applied voltage for the 27d to 27g transition in potassium. A quadratic fit is used to find the voltage at which the frequency is maximized, which is the voltage that nulls the field in the x-direction.

Plotting frequency as a function of applied voltage (Figure 9) allows us to find the voltage at which the field is nulled in that direction and the frequency at that voltage. Once we find the nulling voltage in one direction, we apply it to the rods and move on to the next direction. This way, once we have found the nulling voltage in all three directions, we will have measured the zero-field frequency of the transition.

2.5 Single Photon Excitation to the *g*- and *h*-states

Quantum mechanical selection rules forbid transitions in which the azimuthal quantum number *l* changes by more than one, meaning that these transitions have zero probability. This would normally apply to any *nd* to *ng* and *nd* to *nh* transitions like the ones in this experiment.

However, in the presence of an external electric field, these transitions have nonzero probability, so they can be observed when there is a nonzero electric field. The challenge, then, is to determine the zero-field frequency of the transition by making measurements in a non-zero field. This can be done by interpolation [3]. The process of finding the zero-field frequency is similar to that of the *d* to *f* transitions. We use the *d* to *f* measurement to null the field as much as possible, then adjust the applied voltages in only one direction for the *d* to *g* or *d* to *h* transition. This way, we can obtain a plot of frequency versus voltage as in Figure 9. If the field is close enough to zero, we observe that there is a range of values of applied voltage in the final direction for which the signal is too weak to observe the transition (Figure 10).

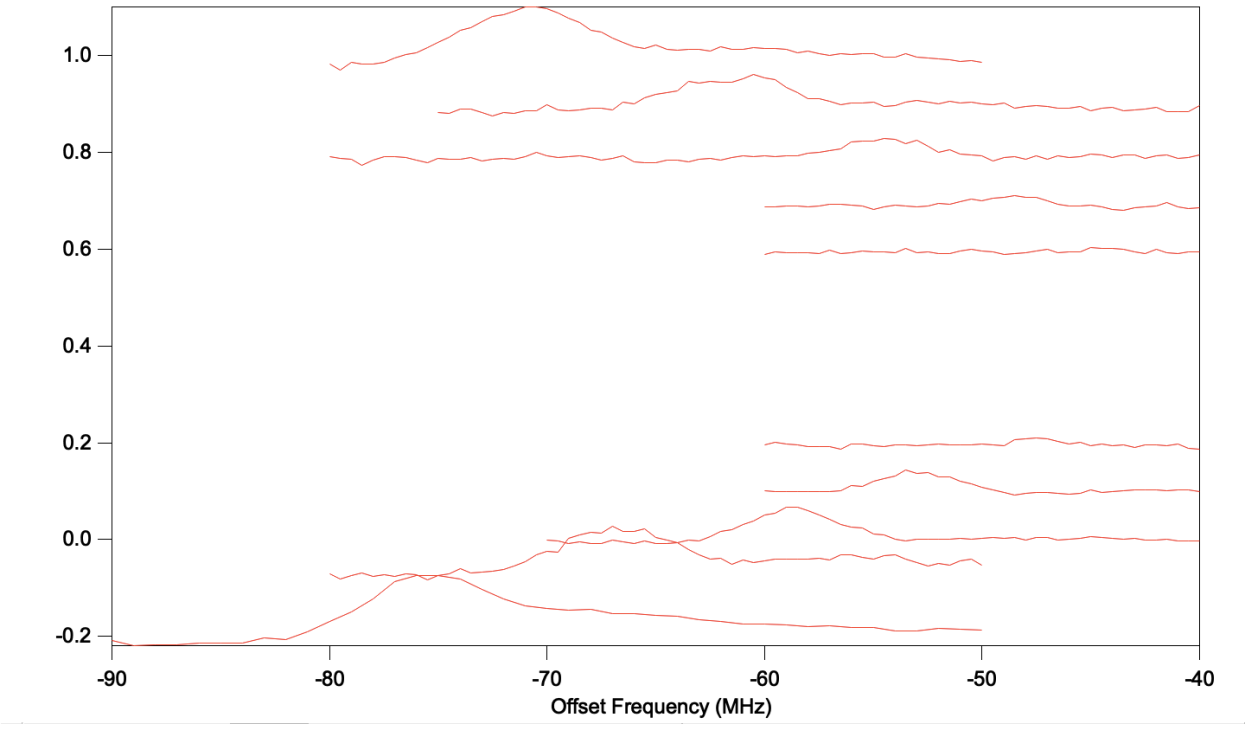

Figure 10: Traces of spectra of the 29d to 29h transition of potassium. The spectra are offset by 0.1 on the y-axis for a difference of 0.4 Volts in applied voltage Vsum. The highest trace corresponds to Vsum = -15V, and the lowest has Vsum = -11.4. For values of Vsum that come close to nulling the field, the transition does not occur or is too weak to observe because the transition is "forbidden" when the external field is zero. In order to find the zero-field frequency, it is necessary to interpolate as shown in Figure 12.

When we apply values of V_{sum} that null the field, the spectra look like flat lines because the transition does not occur. This is due to the fact that the quantum mechanical selection rules

apply when the field is zero. We take multiple frequency measurements on either side of this range and interpolate between the data using a quadratic fit in order to find the peak frequency (Figure 11).

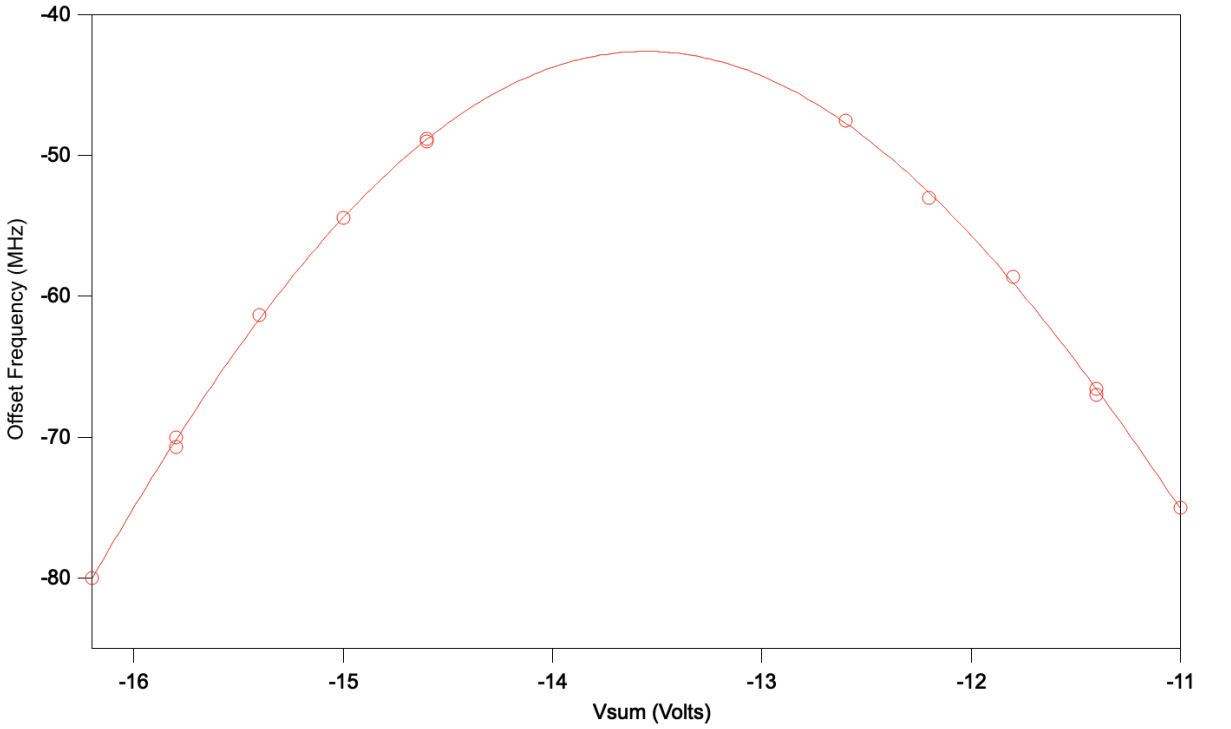

Figure 11: Interpolation using a quadratic fit to find the zero-field frequency of the 29d to 29h transition. Measurements at the peak frequency cannot be made because selection rules forbid this transition when the static electric field is zero. Nonetheless, frequency measurements on both sides of the peak create a well-defined parabola that predicts the zero-field frequency.

3 Results and Discussion

The measured frequencies ν_{df}, ν_{dg}, and ν_{dh} of the $d \rightarrow f$, $d \rightarrow g$, and $d \rightarrow h$ millimeter wave transitions from are displayed in Table 1.

n	ν_{df} (MHz)	ν_{dg} (MHz)	ν_{dh} (MHz)
26	101319	103947	
27	90394	92741	93241
28	81090	83194	
29	72922	74817	75226

Table 1: Measured frequencies of the d to f, d to g, and d to h millimeter wave transitions.

The quantum defects were extracted from the measured zero-field frequencies according to equations (4), (5), and (6). Figure 12 and Table 2 display our measurements alongside theoretical predictions.

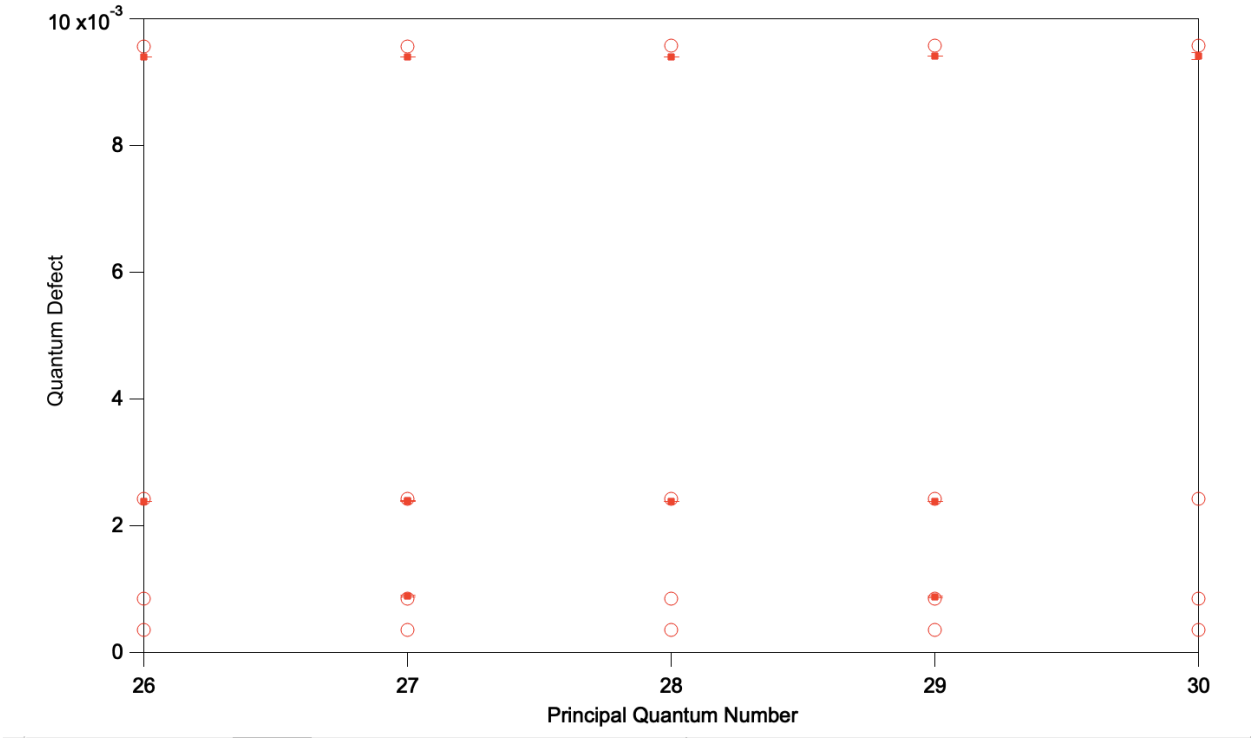

Figure 2: The quantum defects of the f (top), g, h, and i (bottom) Rydberg states of potassium with principal quantum number between 26 and 30. The solid boxes mark measured values and the circles denote theoretical predictions. The measured and theoretical values look close but are inconsistent with each other.

f-states			
n	δ_{theory} (10^{-3})	$\delta_{measured}$ (10^{-3})	$\delta_{theory} - \delta_{measured}$ (10^{-3})
26	9.564	9.395 ± 0.0027	0.169
27	9.568	9.402 ± 0.0030	0.166
28	9.573	9.401 ± 0.0033	0.172
29	9.576	9.415 ± 0.0037	0.161
30	9.580		

g-states			
n	δ_{theory} (10^{-3})	$\delta_{measured}$ (10^{-3})	$\delta_{theory} - \delta_{measured}$ (10^{-3})
26	2.425	2.381 ± 0.0040	0.044
27	2.427	2.387 ± 0.0060	0.040
28	2.428	2.387 ± 0.0050	0.041
29	2.430	2.393 ± 0.0037	0.037
30	2.431		

h-states			
n	δ_{theory} (10^{-4})	$\delta_{measured}$ (10^{-4})	$\delta_{theory} - \delta_{measured}$ (10^{-4})
26	8.516		
27	8.525	8.801 ± 0.220	-0.276
28	8.534		
29	8.541	8.917 ± 0.120	-0.376
30	8.548		

Table 2: Theoretical and measured values of the quantum defects for the f, g, and h states of potassium. The differences between the predicted and measured values are larger than the uncertainties in the measurements in all cases, indicating that measurement and theory are inconsistent.

Theoretical predictions of the *f*-, *g*-, and *h*-states show significant disagreement with our measurements (Table 2). Although the predicted and measured values are clearly in the vicinity of each other, the difference between them is larger than the uncertainty in the measurements. The measurements of the *f*- and *g*-state defects are less than the predicted values, while those for the *h*-state are greater than predicted values. The predicted values for the quantum defects were calculated using equation (2) and theoretical polarizability values for potassium. The polarizability values were calculated from the wavefunctions of potassium using perturbation theory [6].

The largest source of uncertainty in the experiment comes from the fact that the electric field inside the MOT is non-uniform, so it can only be exactly zero at a single point. The MOT cloud has non-zero size, however, so the electric field has some spatial dependence within the cloud. Therefore, the energy difference of a transition between states cannot have the same value for all atoms in the cloud because atoms in slightly different locations will experience slightly different Stark shifts. This leads to the broadening of spectra because the resonant millimeter wave frequency will have a range of values based on the range of Stark shifts. The wider a spectrum is, the less certain we can be about the exact location of the peak, which leads to uncertainty in the frequency.

As the azimuthal quantum number increases, so does the uncertainty in our measurements. This happens for two main reasons. First, we need to interpolate between measurements to find the zero-field frequencies for the *g*- and *h*-states. Even though the transitions to these states do occur in an electric field, they aren't driven as strongly as the *f*-states, so the signal is not as clear, resulting in wider spectra and therefore higher uncertainty in the measured frequency. Second, the polarizability increases with angular momentum. As demonstrated in equation (9), the magnitude of the Stark shift is directly related to the polarizability of the state, so stray fields have a larger impact on the frequency measurements for higher angular momentum.

The stray electric field inside the MOT has the tendency to shift over time. This commonly happens within a matter of hours or even minutes (albeit much more rarely). We aren't sure of the exact cause for this. A leading hypothesis is that charge builds up on the surfaces of the vacuum chamber. When the atoms are ionized, the electrons are accelerated to the microchannel plate detector, but the positive ions move in the opposite direction, possibly

colliding with the insulating wall and building up over time. Regardless of the reason, this phenomenon makes it difficult to fully cancel the field. By nulling the field in one direction at a time, we rely on the field remaining the same after we make our adjustments. This is rarely the case. When we conduct measurements for the *g*- and *h*-state transitions, we look for the values of applied voltage for which we cannot observe the transition, because this would mean that we have gotten very close to an electric field of zero. However, it commonly happens that when we are working on nulling the field in the third direction, we can observe the transition at the peak of the frequency vs voltage graph, as in Figure 10. This means that we haven't nulled the field, because if the field were really zero, we wouldn't be able to observe the transition. In the time it takes to cancel the field in the first two directions and move on to the third direction, the field in one or both or the first two directions has shifted.

Our measurements rely on the field being exactly zero, because otherwise the frequency we measure will be lower than the zero-field frequency. If the frequency we measure is less than the zero-field frequency, the calculation of the quantum defect based on that frequency will yield a result that is too large. This phenomenon, then, does not account for the difference in predicted values with our measurements for the *f*- and *g*-states because the predicted values are larger than the measured ones. In fact, we would expect our quantum defect measurements to be slightly higher than the theoretical values if the theoretical values were correct. This leads us to suspect that the calculated polarizabilities from which we extracted the theoretical quantum defects may be too low. For the *h*-states, the effect of stray field is much larger than it is for the *f*- and *g*-states. This likely accounts for the fact that the measurements of the *h*-state quantum defects are higher than the theoretical values but those for the *f*- and *g*-states are lower.

4 Conclusion

We were able to measure the quantum defects for high angular momentum Rydberg states of potassium. The disagreement between our measurements and theory reveals that the theoretically calculated polarizabilities of potassium may be too low. Nulling the electric field inside the vacuum chamber was the biggest experimental challenge in conducting this measurement due to the unpredictable time-dependence of the stray field. A physical improvement to our experimental field nulling setup would help a great deal in improving upon this method.

References

[1] Philip M. Adamson. “Resonant Collisions of Potassium Atoms.” Colby College Honors Thesis (2016).

[2] Freeman, R. R., and Daniel Kleppner. “Core polarization and quantum defects in high-angular-momentum states of alkali atoms.” Physical Review A 14.5, p1614-1619 (1976).

[3] Lee, J., Nunkaew, J., and T. F. Gallagher. “Microwave spectroscopy of the cold rubidium $(n + 1)d_{5/2} \rightarrow ng$ and nh transitions.” Physical Review A 94, 022505 (2016).

[4] Mayer, J. E., and M. G. Mayer. “The Polarizabilities of Ions from Spectra.” Physical Review Volume 43, p605-611 (1933).

[5] Young, Hugh D. *Statistical Treatment of Experimental Data: An Introduction to Statistical Methods.* Waveland Press, Inc., p99 (2017).

[6] Safronova, U. I., and M. S. Safronova. “High accuracy calculation of energies, lifetimes, hyperfine constants, multipole polarizabilities, and blackbody radiation shift in ^{39}K.” Physical Review A 78, 052504 (2008).